Earth and Planetary Science Letters 538 (2020) 116235

Contents lists available at ScienceDirect

Earth and Planetary Science Letters

www.elsevier.com/locate/epsl

Experimental stabilization of carbonate sediments to calcite: Insights into the depositional and diagenetic controls on calcite microcrystal texture

Mohammed S. Hashim *, Stephen E. Kaczmarek

Department of Geological and Environmental Sciences, Western Michigan University, Kalamazoo, MI 49008, United States

ARTICLE INFO

Article history:
Received 22 October 2019
Received in revised form 4 March 2020
Accepted 13 March 2020
Available online xxxx
Editor: I. Halevy

Keywords:
experiment
carbonate diagenesis
stabilization
calcite crystal
texture

ABSTRACT

Aragonite and high-magnesium calcite are abundant constituents of modern shallow marine carbonate sediments, but are rare in ancient carbonate rocks. Because these minerals are metastable, they tend to stabilize to microcrystalline calcite which is ubiquitous in most Phanerozoic marine and lacustrine limestones. Calcite microcrystals exhibit a range of textures that have been classified in terms of crystal size, morphology, and contact geometry. These textures have the potential to reveal information about the precursor sediments as well as the diagenetic conditions of stabilization, and thus may serve as a proxy for paleoenvironmental conditions. However, despite their ubiquity and importance, the origin of these textures is controversial. Hypotheses regarding the origin of calcite microcrystal textures typically involve inferences regarding the precursor depositional sediments, diagenetic conditions of stabilization, or diagenetic processes. Here, hundreds of laboratory experiments were conducted in which metastable carbonate sediments were stabilized to calcite. The goal of these experiments was to investigate the depositional and diagenetic controls on calcite microcrystal textures. The depositional variables investigated were precursor mineralogy, type, and size, and the diagenetic variables were temperature, fluid chemical composition, and fluid:solid ratio. Our results show that experimental stabilization of carbonate sediments produces calcite with a wide variety of textures depending on the various depositional and diagenetic parameters. These textures are remarkably similar to those commonly observed in the rock record. Calcite microcrystal morphology is controlled by fluid chemistry, fluid:solid ratio, and reactant type. Calcite microcrystal size is controlled by temperature, fluid chemistry, fluid:solid ratio, and reactant size. The degree to which calcite microcrystals are fitted together is controlled by reactant size and reactant microstructure. Our findings challenge most of the existing hypotheses regarding the origin of calcite microcrystal textures. We specifically show that textures that have been interpreted to indicate late diagenetic processes such as dissolution and cementation, may be the result of the early diagenetic processes of stabilization.

1. Introduction

Aragonite and high-magnesium calcite (HMC) are the most abundant carbonate minerals in modern shallow marine sediments, but extremely rare in ancient limestones (Morse and Mackenzie, 1990). The rarity of these minerals in the geologic record is attributed to their metastability (Bathurst, 1975). That is, though aragonite and HMC precipitate more readily in marine waters due to kinetic factors (Morse et al., 2007), they are thermodynamically less stable than low-Mg calcite (calcite) under Earth's surface conditions. As a result, one of the early diagenetic alterations aragonite and HMC may experience is dissolution, often immediately followed by precipitation of microcrystalline calcite cement, a process referred to as stabilization (Milliman, 1974; Casella et al., 2017).

Stabilization to calcite microcrystals is an important and ubiquitous diagenetic process (Kaczmarek et al., 2015). Ancient limestones are routinely used to reconstruct the history of Earth's surface conditions, and global geochemical cycles (e.g., Sandberg, 1983), despite the observation that stabilization can significantly alter isotopic and trace elemental signatures (e.g., Ahm et al., 2018). Furthermore, stabilization is generally accompanied by complete rearrangement of the pore system as the heterogeneous assortment of carbonate sediments is altered to a homogeneous collection of calcite microcrystals (e.g., Moshier, 1989).

* Corresponding author.
E-mail address: m_acg@icloud.com (M.S. Hashim).

https://doi.org/10.1016/j.epsl.2020.116235
0012-821X/

Diagenetic calcite microcrystals typically measure between 1–9 μm and are common throughout matrix and allochems in ancient limestones (e.g., Loucks et al., 2013). Various textural classifications have been proposed for calcite microcrystals based on physical attributes, such as crystal size, morphology, and contact geometry (e.g., Moshier, 1989; Deville de Periere et al., 2011; Kaczmarek et al., 2015). In general, three main microcrystal textures have been observed across a wide range of geologic ages, depositional settings, burial depths, and precursor types. Detailed descriptions of the calcite microcrystal textural classes are provided in Kaczmarek et al. (2015). Volumetrically, the two most abundant microcrystal textures are the granular (framework) and fitted (mosaic) textures (Moshier, 1989; Kaczmarek et al., 2015). The granular texture is defined as a loose framework of microcrystals, and is further subdivided into granular euhedral and granular subhedral subclasses based on crystal shape (Kaczmarek et al., 2015). The fitted texture is a compact mosaic of interlocking microcrystals exhibiting mostly curvilinear compromise boundaries and very little pore space. Fitted is further subdivided into fitted-partial and fitted-fused based on a combination of packing, interfacial angles between crystals, and intercrystal porosity (Kaczmarek et al., 2015). The term microcrystal, as used here, broadly refers to any micrometer-scale low-magnesium calcite mineral crystal (Kaczmarek et al., 2015), and includes both micrite and microspar.

Whereas the vast majority of textural and geochemical evidence suggests that calcite microcrystals form through diagenetic stabilization of metastable sediments (Hasiuk et al., 2016 and references therein), a recent literature review suggests that no consensus exists regarding the origin of the various calcite microcrystal textures (Hashim and Kaczmarek, 2019). Multiple hypotheses have been proposed (e.g., Longman and Mench, 1978; Moshier, 1989; Loucks et al., 2013), but all suffer from limited observations. Some explanations suggest that calcite microcrystal textures are determined by depositional parameters, such as the mineralogy or texture of the precursor sediments (Longman and Mench, 1978; Lasemi and Sandberg, 1993; Deville de Periere et al., 2011). Others, in contrast, ascribe textures to the diagenetic conditions during stabilization, such as fluid:solid ratio (Moshier, 1989) or fluid chemistry (Folk, 1974). Still others have invoked specific diagenetic processes, such as dissolution and compaction (Lambert et al., 2006; Volery et al., 2010). Moshier (1989), for example, suggested that the granular texture reflects stabilization in low fluid:solid ratio (i.e., closed system), whereas the fitted texture indicates stabilization in high fluid:solid ratio (i.e., open system). In contrast, Lambert et al. (2006) proposed that granular subhedral (rounded) calcite microcrystals indicate partial dissolution of granular euhedral microcrystals during burial diagenesis, and that the fitted texture indicates cementation during burial compaction.

In modern natural environments, Steinen (1982) observed euhedral (rhombic) calcite microcrystals among Holocene aragonitic sediments. Experimental observations by McManus and Rimstidt (1982) showed that aragonite needles stabilize to euhedral calcite microcrystals. These observations provide the basis for the general hypothesis that the granular euhedral texture forms first during mineralogical stabilization of metastable sediments (e.g., Lambert et al., 2006; Loucks et al., 2013). In ancient limestones, however, it is difficult to determine the controls on calcite microcrystal textures for multiple reasons. First, the precursor sediments from which calcite microcrystals stabilize are characterized by diverse textures and minerals that can vary spatially (e.g., Gischler et al., 2013) and temporally (e.g., Sandberg, 1983). Second, stabilization must occur under a wide range of diagenetic conditions, such as fluid chemistry and hydrodynamics (Moshier, 1989). Third, stabilization can be followed by further diagenesis that may alter the mineralogy (i.e., dolomitization), texture, and original geochemical signatures (e.g., Lambert et al., 2006). To overcome these challenges, laboratory experiments have been employed to explore stabilization of metastable sediment to calcite. The benefit of laboratory experiments is that geochemical parameters can be controlled rather than inferred. Numerous studies, for example, have investigated various aspects of the aragonite to calcite transition, including reaction rate (e.g., Bischoff, 1969), reaction mechanism (e.g., McManus, 1982; Perdikouri et al., 2013), kinetic inhibitors and catalysts (e.g., Bischoff and Fyfe, 1968), and isotopic variations (e.g., Ritter et al., 2017; Guo et al., 2019). However, the textural aspects of stabilization have received far less attention.

McManus and Rimstidt (1982) reported in a GSA conference abstract, later published by Moshier (1989), that synthetic aragonite needles in distilled water stabilize to calcite microcrystals at 50 °C and 1 bar. In an unpublished Ph.D. dissertation, Papenguth (1991) conducted dozens of stabilization experiments using synthetic and natural reactants. He observed that stabilization occurs by dissolution of metastable sediments and precipitation of calcite as cement, and that calcite crystal size does not change with extended reaction time. The main drawback of this study, however, is the lack of systematic control. That is, multiple variables were changed between experiments.

Studies that systematically evaluated the controls on calcite microcrystal textures are rare. Accordingly, many of the questions regarding the origin of these textures remain unanswered. Specifically, what are the controls on calcite microcrystal textures? Do these textures reflect specific depositional or diagenetic conditions? In other words, can the depositional characteristics of precursor sediment or the diagenetic conditions of stabilization be inferred from calcite microcrystal textures? To address these questions, hundreds of laboratory experiments were conducted, and their results and implications to natural stabilization are discussed here.

2. Methods

All laboratory stabilization experiments presented here involve the conversion of a metastable carbonate mineral reactant (either aragonite (A) or high-Mg calcite (HMC)) to low-magnesium calcite (C) in an aqueous solution. These dissolution–precipitation reactions are represented by Equations (1) and (2):

$$CaCO_{3\ (A)} \rightarrow Ca^{2+}{}_{(aq)} + CO_3^{2-}{}_{(aq)} \rightarrow CaCO_{3\ (C)} \quad (1)$$

$$Ca_{(1-x)}Mg_{(x)}CO_{3\ (HMC)} \rightarrow Ca^{2+}{}_{(aq)} + Mg^{2+}{}_{(aq)} + CO_3^{2-}{}_{(aq)} \rightarrow CaCO_{3\ (C)} \quad (2)$$

Controlled experiments were specifically designed to test the effect of specific depositional and diagenetic variables on calcite microcrystal textures. The depositional variables investigated include reactant mineralogy (aragonite vs. HMC), reactant type (synthetic, biogenic, non-biogenic, etc.), and reactant size fractions. The diagenetic variables were temperature, fluid:solid ratio, and fluid chemistry. Experimental conditions for each set of experiments are presented in Table 1. Experimental Series 1 stabilized 0.1 g of single crystal aragonite that was pulverized and sieved to obtain $<$63 μm size fraction at 100 °C in 15 ml of deionized (DI) water. In subsequent series, all experimental variables were held constant except for the variable of interest. Series 2 tested reaction temperature, Series 3 fluid:solid ratio, Series 4 fluid chemistry, Series 5 reactant type and mineralogy, and Series 6 reactant size (Table 1). It should be noted that each one of these series includes multiple experiments conducted for various periods of time, and that at least one experiment in each series was run in duplicate (supplemental table S1).

All stabilization reactions were performed in Teflon-lined stainless steel acid digestion vessels charged with solid and fluid re-

Table 1
Experimental conditions.

Experiment series	Temperature (°C)	Solution volume (mL)/solid weight (g)	Solution chemistry (mM)	Reactant type	Reactant size (μm)	Time to >90% calcite product (h)
1	100	15/0.1 = 150	Deionized (DI) water	Single crystal aragonite (SCA)	<63	120
2-1	50	15/0.1 = 150	DI	SCA	<63	2000
2-2	70	15/0.1 = 150	DI	SCA	<63	700
2-3	150	15/0.1 = 150	DI	SCA	<63	71
2-4	200	15/0.1 = 150	DI	SCA	<63	72
3-1	100	5/0.1 = 50	DI	SCA	<63	144
3-2	100	1/0.1 = 10	DI	SCA	<63	120
3-3	100	0.1/0.1 = 1	DI	SCA	<63	74
3-4	100	0.35/0.44 = 0.8	DI	SCA	<63	48
3-5	100	0.35/0.44 = 0.8	DI	Synthetic aragonite (SA)	<63	–
4-1	100	15/0.1 = 150	[NaCl] = 546	SCA	<63	48
4-2	100	15/0.1 = 150	[NaCl] = 469	SCA	<63	48
4-3	100	15/0.1 = 150	[KCl] = 10.2	SCA	<63	120
4-4	100	15/0.1 = 150	[$CaCl_2$] = 10.3	SCA	<63	48
4-5	100	15/0.1 = 150	[$CaCl_2$] = 45	SCA	<63	36
4-6	100	15/0.1 = 150	[Na_2SO_4] = 28	SCA	<63	548
4-7	100	15/0.1 = 150	[$MgCl_2$] = 55	SCA	<63	–
4-8	100	15/0.1 = 150	Seawater (SW)	SCA	<63	–
4-9	100	15/0.1 = 150	SW w/Mg/Ca = 1	SCA	<63	–
5-1	100	15/0.1 = 150	DI	SA	<63	100
5-2	100	15/0.1 = 150	DI	Gastropods	<63	680
5-3	100	15/0.1 = 150	DI	Corals	<63	–
5-4	100	15/0.1 = 150	DI	Ooids	<63	–
5-5	200	15/0.1 = 150	DI	Corals	<63	1000
5-6	200	15/0.1 = 150	DI	Ooids	<63	1000
5-7	200	15/0.1 = 150	DI	Corals	~5000	480
5-8	200	15/0.1 = 150	DI	Ooids	212-250	480
5-9	200	15/0.1 = 150	DI	*Halimeda*	~5000	720
5-10	200	15/0.1 = 150	DI	*Halimeda*	<63	720
5-11	200	15/0.1 = 150	DI	*Penicillus*	–	720
5-12	200	15/0.1 = 150	DI	*Jania rubens*	<63	–
5-13	200	15/0.1 = 150	DI	*Lithothamnion*	<63	–
5-14	200	15/0.1 = 150	DI	*Goniolithon*	<63	–
6-1	100	15/0.1 = 150	DI	SCA	90-106	500
6-2	100	15/0.1 = 150	DI	SCA	8-20	–
6-3	100	15/0.1 = 150	DI	SCA	<8	–

actants. Sealed reaction vessels were placed into pre-heated convection ovens set to a fixed temperature for predetermined times. Upon removal, reaction vessels were immediately cooled to room temperature with forced air. Solid and fluid contents were then separated using a vacuum flask. Solid contents were rinsed in DI water and dried in a vacuum desiccator. Liquids were discarded.

Natural reactants used in the experiments were single crystal aragonite, aragonitic ooids from Ambergris Cay, aragonitic corals, *Halimeda*, *Penicillus*, *Lithothamnion*, *Goniolithon* from the Bahamas, and gastropods and *Jania rubens* from Qatar. An agate mortar and pestle were used to pulverize reactants to be used in some of the experiments. The powders were then dry sieved using either U.S. standard stainless sieve to obtain the <63 μm size fraction, or nylon mesh screen discs to obtain 20–8, and <8 μm size fractions. Natural reactants were chemically treated with sodium hypochlorite (NaClO) and hydrogen peroxide (H_2O_2) to remove organic matter (for details see supplemental material). In addition to the natural reactants, aragonite needles were synthesized using the methods of Wray and Daniels (1957) as modified by Katz (1973) (for details see supplemental material).

Reaction solutions were prepared using reagent grade salts and DI water. Synthetic seawater with 35‰ salinity was prepared following the method described by Millero (2016). Synthetic seawater was modified by adding $CaCl_2$ to obtain Mg/Ca ratio of 1 representative of seawater during geologic times of "calcite seas" (e.g., Lowenstein et al., 2001). Ionic solutions were prepared using salts to represent the six major ions (Cl^-, Na^+, Mg^{2+}, SO_4^{2-}, Ca^{2+}, and K^+) in modern seawater with their respective molarity (mmol l^{-1}): NaCl = 546, and = 469; $MgCl_2$ = 55; Na_2SO_4 = 28; $CaCl_2$ = 10.3; and KCl = 10.2. A solution with $CaCl_2$ = 45 mM was also prepared.

The highest fluid:solid ratio (15 mL:0.1 g) used represents stabilization in a fluid dominated setting (e.g., sediment water interface), whereas the lowest ratio (0.35 mL:0.44 g) represents stabilization of sediments with 70% porosity in a closed system (e.g., shallow burial setting). The 70% porosity represents the typical porosity of shallow marine carbonate mud (e.g., Kominz et al., 2011). This fluid:solid ratio was calculated using Equation (3), and assuming an aragonite density of 2.93 g/cm^3.

$$\frac{\text{fluid}}{\text{solid}} = \frac{\text{porosity}}{(1-\text{porosity}) * \text{density}} \tag{3}$$

Standard powder XRD techniques were used to determine the mineralogy of all solids. Powders were prepared with an agate mortar and pestle. Powders were then mounted on a Boron-doped silicon P-type zero background diffraction plates and placed in a Bruker D2 Phaser Diffractometer with a Cu$K\alpha$ anode. Relative abundances of aragonite, low-Mg calcite, and HMC were determined using the ratio of aragonite 111 and calcite 104 reflection intensities (Milliman, 1974).

Scanning electron microscope imaging was performed on a JEOL 7500F, JEOL 6610LV, or JEOL IT100. The accelerating voltage was 20 kV and the working distance was 10 mm. Samples were coated with either 10 nm of osmium, 30 nm of gold, or 30 nm of carbon.

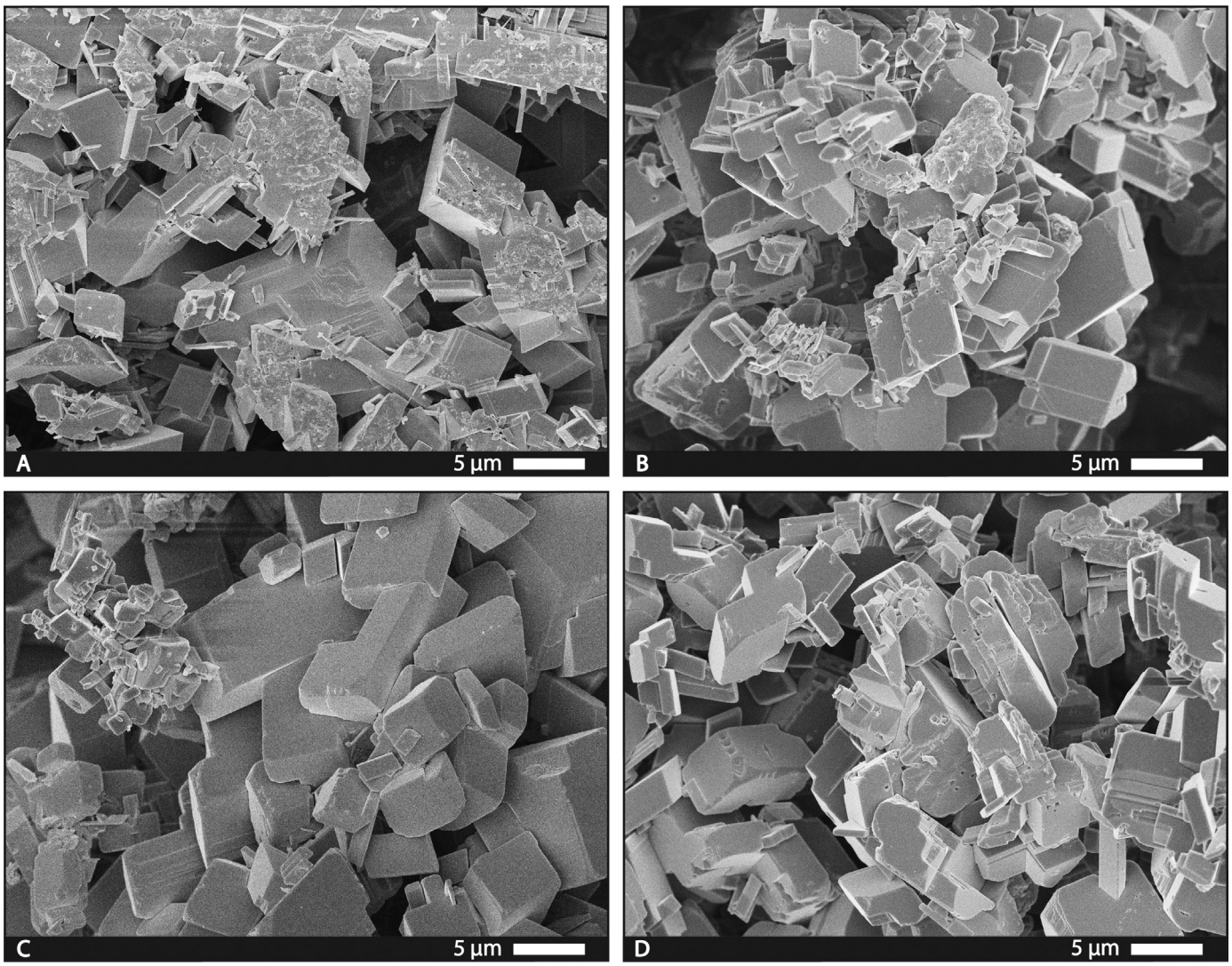

Fig. 1. SEM photomicrographs from Series 1 showing calcite microcrystals exhibiting granular euhedral texture at various reaction times. (A) After 70 h. (B) 500 h. (C) 1000 h. (D) 4980 h. All experimental conditions are presented in Table 1.

Crystal size measurements were performed using either the measurement tool equipped with the JEOL IT100 SEM or Jmicrovision software v1.3.1 (Roduit, 2007).

3. Results

The compiled results from all stabilization experiments are presented in supplemental Table S1. Aragonite reactants in Series 1 invariably stabilize to calcite microcrystals exhibiting the granular euhedral texture (Fig. 1). Extended reaction time showed no effect on calcite microcrystal texture (Fig. 1). Slight changes in calcite average crystal size (ACS) were documented with increased reaction time, but no trend between ACS and reaction time over the period of investigation was observed (Fig. 2a, and supplemental Fig. S1).

Higher reaction temperatures in Series 2 correlate with faster reaction rates (Fig. 3a) and smaller ACS (Fig. 2b). All calcite microcrystals in Series 2 exhibit the granular euhedral texture (Fig. 4).

Lower fluid:solid ratios in Series 3 correlate with faster reaction rates (Fig. 3b). All calcite microcrystals in Series 3 exhibit the granular texture (Fig. 5), but lower fluid:solid ratio experiments are associated with a higher proportion of anhedral and subhedral calcite microcrystals (Fig. 5). Lower fluid:solid ratios yield smaller calcite microcrystals compared to Series 1. In Series 3-1 and 3-2 (Table 1), aragonite stabilizes to euhedral calcite microcrystals, whereas in Series 3-3 and 3-4, aragonite stabilizes to a mixture of anhedral and subhedral microcrystals. Series 3-4 produced calcite microcrystals with an ACS of 3.71 µm. The majority of the subhedral microcrystals are characterized by rough surfaces and stepped growth faces. Experiments starting with the synthetic aragonite reactants and a fluid:solid ratio of 0.8 (Series 3-5) produce mostly euhedral calcite microcrystals with a few (<10%) anhedral ones (supplemental Fig. S2).

Series 4 results demonstrate that although aragonite stabilization to calcite in NaCl (Series 4-1 and 4-2), KCl (Series 4-3), and $CaCl_2$ solutions (Series 4-4) is faster compared to Series 1 (Fig. 3c), these experiments yield calcite microcrystals characterized by the same granular euhedral texture as in Series 1 (Fig. 6). Experiments conducted in the NaCl solution (Series 4-2) yield calcite microcrystals with ACS of 4.90 µm, which is smaller than Series 1. Experiments conducted in solution containing 45 mM $CaCl_2$ (Series 4-5) yield calcite with granular texture. Individual microcrystals are mostly euhedral, but <5% are polyhedral (Fig. 6d). The polyhedral microcrystals are generally larger than the euhedral microcrystals, but the ACS of Series 4-5 is smaller than Series 1. Both the abundance and polyhedrality (i.e., development of more crystal faces) of microcrystals increase with reaction time.

In contrast to NaCl, KCl, and $CaCl_2$ experiments, reaction rate in the Na_2SO_4 solution (Series 4-6) is slower compared to Series

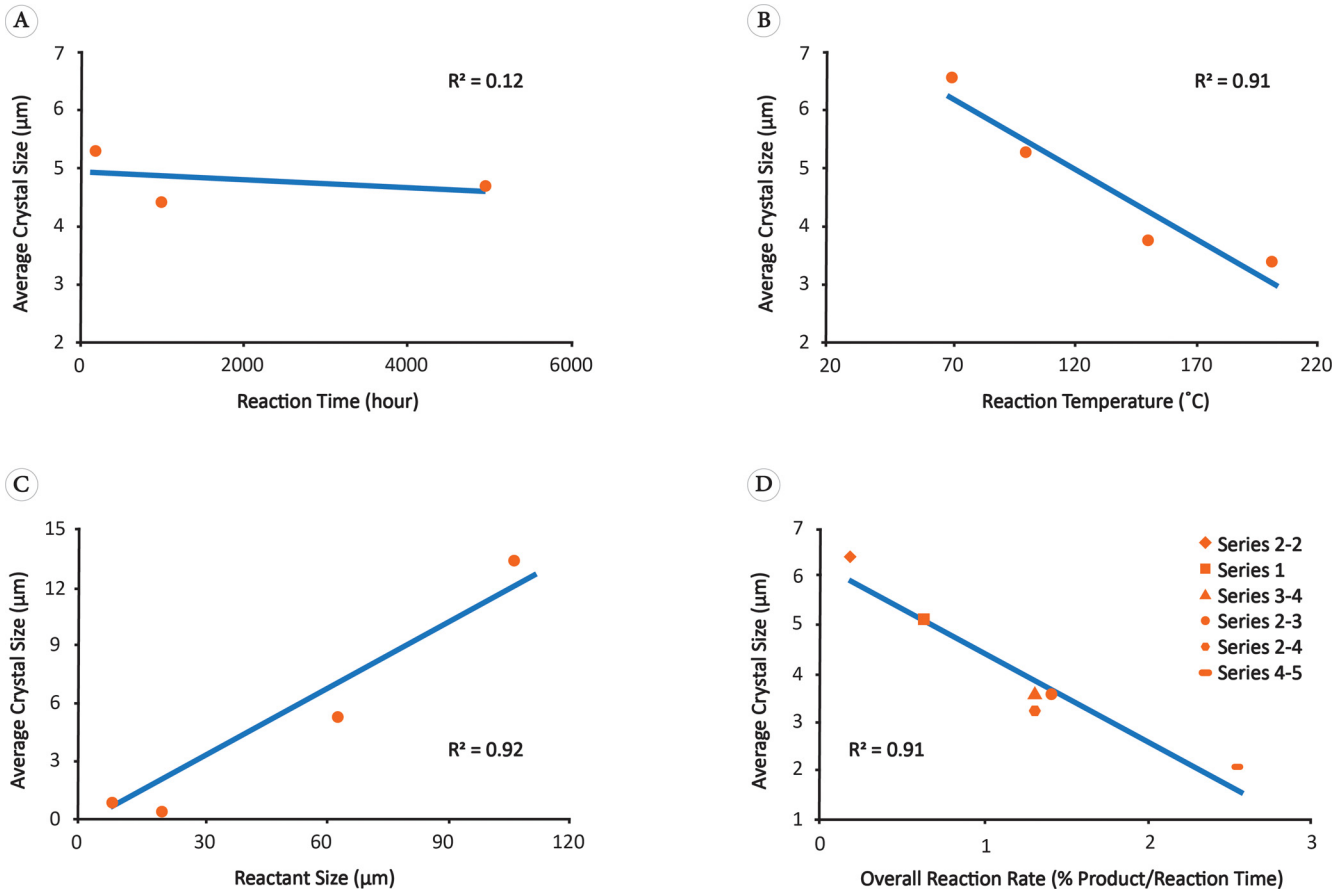

Fig. 2. The relationship between average crystal size of calcite and various experimental parameters. (A) Reaction time (Series 1). (B) Reaction temperature (Series 2). (C) Reactant size (Series 6). (D) Overall reaction rate from Fig. 3 (slope of reaction curves when plotted as calcite product percent vs. reaction time in hour).

1 (Fig. 3c). Calcite microcrystals in Series 4-6 are overwhelmingly subhedral (i.e., polyhedral) (Fig. 6c). In the $MgCl_2$ solution (Series 4-7), no calcite was detected by XRD after 720 h (Fig. 3c). Experiments in synthetic seawater (Series 4-8) formed HMC in small amount (1.2%) after 7 months. In experiments conducted with modified synthetic seawater (Series 4-9), no calcite was detected after 7 months.

The synthetic aragonite in Series 5-1 stabilizes to calcite faster compared to Series 1 (Fig. 3d) and produces calcite microcrystals with granular euhedral texture (Fig. 7a). Gastropods (Series 5-2) stabilize to calcite slower compared to Series 1 (Fig. 3d), and produces calcite microcrystals with granular subhedral texture (Fig. 7b). Compared to Series 1, however, the calcite microcrystals in Series 5-2 are more closely packed. Corals and ooids are slower to stabilize to calcite compared to Series 1 (Fig. 3d). After 1 year at 100 °C, only 30% of coral (Series 5-3) and ooid (Series 5-4) reactants stabilize to calcite. At 200 °C, in contrast, >95% of coral (Series 5-5) and ooid (Series 5-6) reactants stabilize to calcite after 1000 h (41 days). Calcite microcrystals from Series 5-5 and 5-6 are characterized by granular subhedral texture (Fig. 7c and 7d) and exhibit a bimodal ACS, where both microcrystal populations are subhedral (i.e., polyhedral), but smaller microcrystals are typically more polyhedral.

Whole (unpowdered) coral fragments (Series 5-7) and ooids (Series 5-8) stabilize to polyhedral calcite microcrystals with fitted-partial texture (Fig. 8a and 8b). Some crystals are > 10 μm, but the majority are microcrystals measure <10 μm. The calcite microcrystals on the surfaces of the corals and ooids vary in size (supplemental Fig. S3). *Halimeda* (Series 5-9) stabilizes to polyhedral calcite microcrystals with fitted partial texture (supplemental Fig. S4a), whereas pulverized *Halimeda* (Series 5-10) stabilizes to polyhedral calcite microcrystals with granular texture (supplemental Fig. S4b). Similar to gastropod experiments (Series 5-2), the microcrystals in Series 5-10 appear closer together compared to Series 1, but the texture is granular. Calcite crystals that result from stabilization of *Halimeda* and pulverized *Halimeda* (Series 5-9 and 5-10) are typically >10 μm, but some microcrystals measure <10 μm. *Penicillus* (Series 5-11) stabilizes to calcite microcrystals with fitted partial texture (Fig. 8c). *Jania rubens* (Series 5-12), *Lithothamnion* (Series 5-13), and *Goniolithon* (Series 5-14) (HMC) did not convert to calcite in detectible amounts after 1000 h at 100 °C or 200 °C.

Series 6 results show that smaller reactants stabilize slower compared to Series 1, and broadly correlate with smaller calcite microcrystals (Fig. 2c). Smaller reactants (Series 6-2 and 6-3) produce subhedral microcrystals which exhibit fitted partial texture (Fig. 9).

4. Discussion

The observation that HMC reactants or aragonite in Mg^{2+} bearing solutions at seawater concentration showed no evidence of stabilization to calcite over the period of investigation is consistent with previous experimental studies reporting the failure to stabilize HMC (e.g., Oti and Müller, 1985) or aragonite in Mg^{2+}-solutions (e.g., Bischoff and Fyfe, 1968; Bischoff, 1969; Papenguth, 1991; Guo et al., 2019). The most commonly cited explanation for this phenomenon is the inhibiting effect of Mg^{2+} on stabilization of aragonite and HMC (see review by Hashim and Kaczmarek, 2019). As such, the discussion will focus on the fundamental controls on calcite crystal morphology, crystal size, and degree to which these crystals are fitted together on the aragonite to calcite stabilization in Mg^{2+} free solutions only.

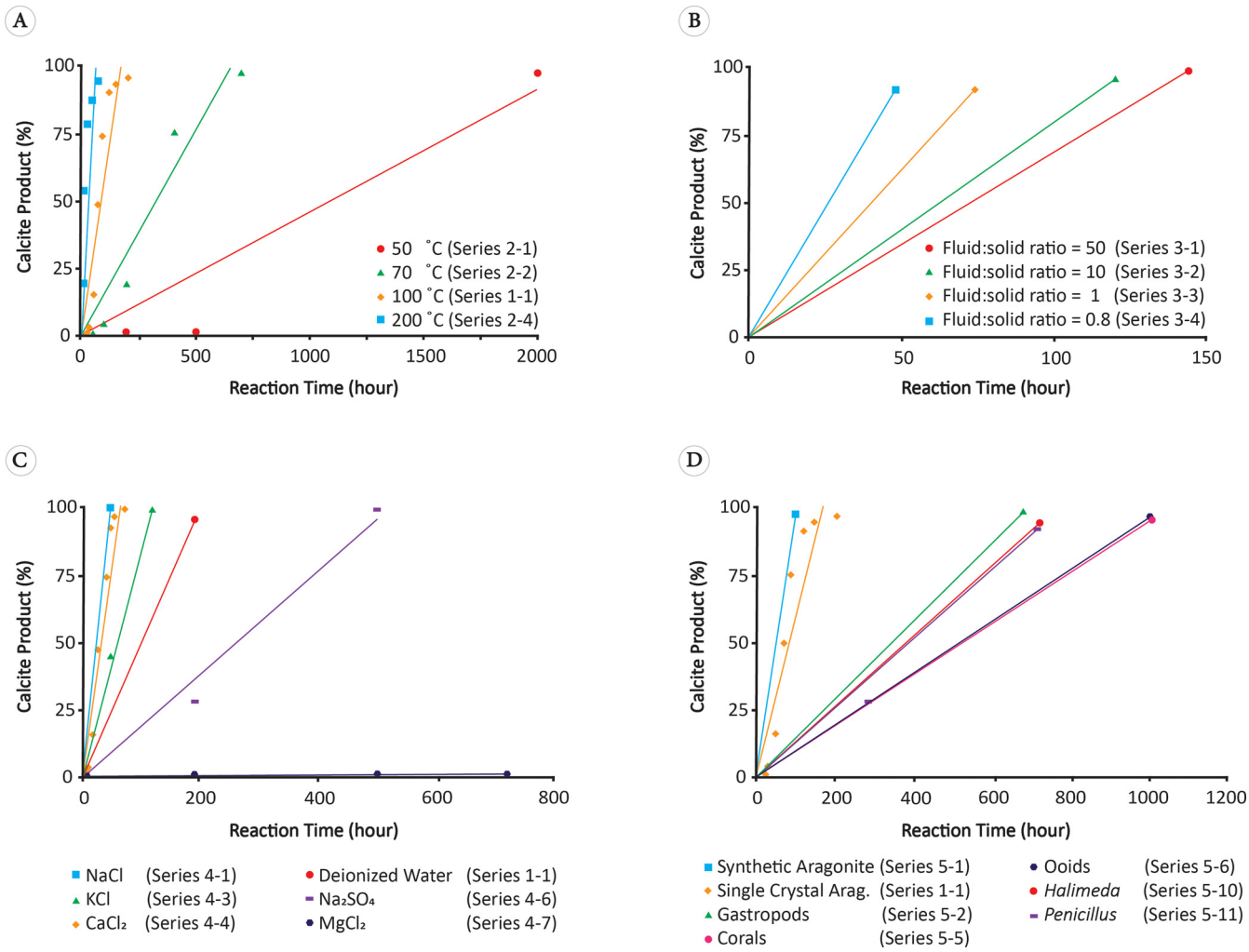

Fig. 3. Dependence of aragonite to calcite reaction rate on various experimental conditions. (A) Temperature (Series 2). (B) Fluid:solid ratio (Series 3). (C) Fluid chemical composition (Series 4). (D) Reactant type (Series 5).

4.1. Controls on calcite microcrystal morphology

In crystallization processes (i.e., precipitation from solution), crystal morphology is primarily determined by crystal system and growth conditions (Sunagawa, 2007). Calcite, for example, belongs to the hexagonal (rhombohedral) crystal system, which allows for a number of crystal forms, most commonly including rhombohedron, prism, and scalenohedron. Among growth conditions that may affect calcite crystal morphology is the presence of chemical species other than Ca^{2+} and CO_3^{2-} in the solution (Fig. 6c), and degree of supersaturation (Fig. 6d). In addition, aragonite to calcite stabilization involves dissolution of the former and precipitation of the latter. As a result, calcite heterogeneously nucleates on the aragonite surface, and crystal lattice ions (Ca^{2+} and CO_3^{2-}) are supplied by dissolution of aragonite reactant. Accordingly, reactant characteristics such as type and surface area, as well as fluid:solid ratio of the system may also affect calcite crystal morphology (Fig. 5, 7, and 8).

4.1.1. Fluid chemistry

The observation that stabilization in the $CaCl_2$ solution produced polyhedral calcite microcrystals (Fig. 6d) can be explained by the increase in the supersaturation with respect to calcite due to the common ion effect (Bischoff and Fyfe, 1968). A change in the degree of supersaturation is accompanied by a change in growth rates of the different crystal surfaces but to different degrees (Sunagawa, 2007), which result in a change in crystal morphology (Fig. 6d). Bosak and Newman (2005) demonstrated that as supersaturation with respect to calcite increases, calcite crystal morphology changes from rhombohedral to framboidal. The effect of supersaturation on crystal morphology is a well-known phenomenon and has also been documented in many minerals (e.g., Sunagawa, 2007).

Mg^{2+} and SO_4^{2-} have been observed to substitute for Ca^{2+} and CO_3^{2-} in the calcite crystal lattice both in experimental and natural settings (Busenberg and Plummer, 1985; Morse, 1986). These ions increase the solubility of calcite, and significantly slow down its growth rate (Bischoff and Fyfe, 1968; Busenberg and Plummer, 1985). More important perhaps, Mg^{2+} and SO_4^{2-} can distort the calcite crystal lattice, which can translate into a change in crystal morphology. The incorporation of SO_4^{2-} and its substitution with CO_3^{2-} explain our observations that stabilization in Na_2SO_4 solution was slower and resulted in polyhedral calcite microcrystals compared to Series 1 (Fig. 6c). In contrast, monovalent ions, such as Na^+ and K^+ have been hypothesized to occupy interstitial positions in calcite crystal lattice because they do not readily substitute for the divalent Ca^{2+} (Ishikawa and Ichikuni, 1984). In this case, incorporated Na^+ and K^+ do not distort crystal structure, and thus no change in crystal morphology occurs. This mode of incorporation is consistent with our observation that stabilization in NaCl and KCl solutions produced euhedral calcite microcrystals similar to those resulted in stabilization in distilled water (compare Fig. 1

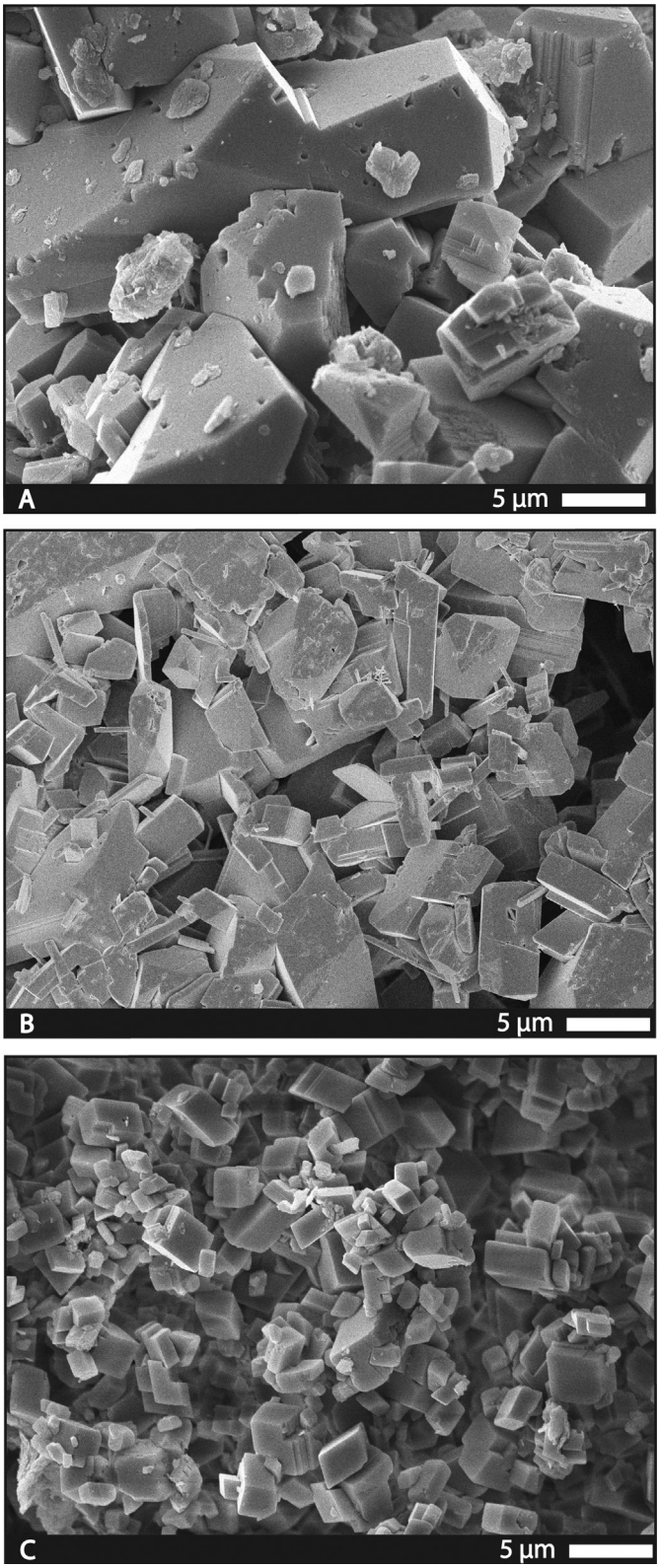

Fig. 4. SEM photomicrographs from Series 2 showing calcite microcrystals from stabilization at various temperatures. (A) 50 °C. (B) 70 °C. (C) 200 °C. Calcite microcrystals at all temperatures exhibit granular euhedral texture.

with Fig. 6a and 6b). These observations suggest that the effect of (impurity) ions on calcite crystal morphology depends on whether the incorporated ions substitute with calcite crystal lattice ions or reside within the lattice.

4.1.2. Fluid:solid ratio

There are multiple explanations for why stabilization experiments in low fluid:solid ratio produce anhedral and subhedral rather than euhedral calcite microcrystals (Fig. 5d). First, the anhedral and subhedral microcrystals may reflect the texture of the single crystal aragonite reactant, which is characterized by anhedral constituents (supplemental Fig. S5a). It has also been suggested that the aragonite to calcite transformation regime (i.e., style) is determined by the fluid:solid ratio (e.g., McManus, 1982; Pederson et al., 2019). Transformation in high fluid:solid ratio occurs via bulk dissolution-reprecipitation, which obliterates reactant texture, whereas transformation in low fluid:solid ratio occurs via thin fluid films, and results in retention of precursor texture (McManus, 1982). However, our results show that stabilization of synthetic aragonite needles in low fluid:solid ratio (Series 3-5 in Table 1) yields anhedral and euhedral microcrystals (supplemental Fig. S2). This observation argues against the idea that calcite microcrystal texture reflects that of the aragonite precursor.

An alternative hypothesis to explain the origin of anhedral and subhedral crystals in the low fluid:solid ratio experiments (Fig. 5c and 5d) involves a competition of growing crystals for space. When crystals grow in aggregation, their morphology is altered by the physical barriers (i.e., other crystals or container walls) that they grow into (Sunagawa, 2007). The effect of crystal competition can be seen in all experiments where crystals grow into each other and their morphologies are altered accordingly (e.g., Fig. 1 and 5). But crystal competition is probably more prominent in the low fluid:solid ratio experiments because growing crystals are more likely to be surrounded by aragonite reactants and other growing calcite crystals than by solvent molecules (Fig. 5d). This interpretation is further supported by the observation that smaller microcrystals that are solitary are also more euhedral compared to larger microcrystals that are surrounded by other crystals (Fig. 5c and 5d).

4.1.3. Reactant type

Although single crystal aragonite and synthetic aragonite reactants have very different textures (supplemental Fig. S5a and S5b), both inorganic reactants invariably stabilize to euhedral calcite microcrystals (Fig. 1 and 7a, respectively). In contrast, natural marine allochems, such as gastropod, coral, *Halimeda*, *Penicillus*, and ooids, despite being characterized by different textures (supplemental Fig. S5), stabilize to polyhedral calcite microcrystals (Fig. 7b, 7c, and 7d) and are characterized by the slowest reaction rates (Fig. 3d). These observations indicate that under the experimental conditions tested, reactant texture does not impact calcite microcrystal texture. Instead, the presence of organic matter in natural marine allochems may be responsible for the retardation of reaction rate, and the formation of polyhedral calcite microcrystals. Organic matter is common in natural waters and in association with carbonate sediments (Morse et al., 2007). Organic matter has been demonstrated to influence reaction kinetics of carbonate minerals (e.g., Jackson and Bischoff, 1971; Morse et al., 2007; Casella et al., 2017) and their crystal morphology (e.g., Bosak and Newman, 2005; Morse et al., 2007). Jackson and Bischoff (1971) investigated the influence of various amino acids commonly found in natural waters (Morse et al., 2007) on the aragonite to calcite reaction rate. They observed that the presence of neutral and basic amino acids accelerated the reaction rate, whereas acidic amino acids retarded it. They attributed the inhibiting effect to the substitution of the extra negatively charged carboxyl group (COOH) for CO_3^{2-} in the calcite crystal lattice. In contrast, basic and neutral amino acids contained only one carboxyl group, which they reasoned was unavailable for substitution due to interaction with an amine group in the amino acid. However, Jackson and Bischoff (1971) did not report on how these organics affected calcite crystal morphology.

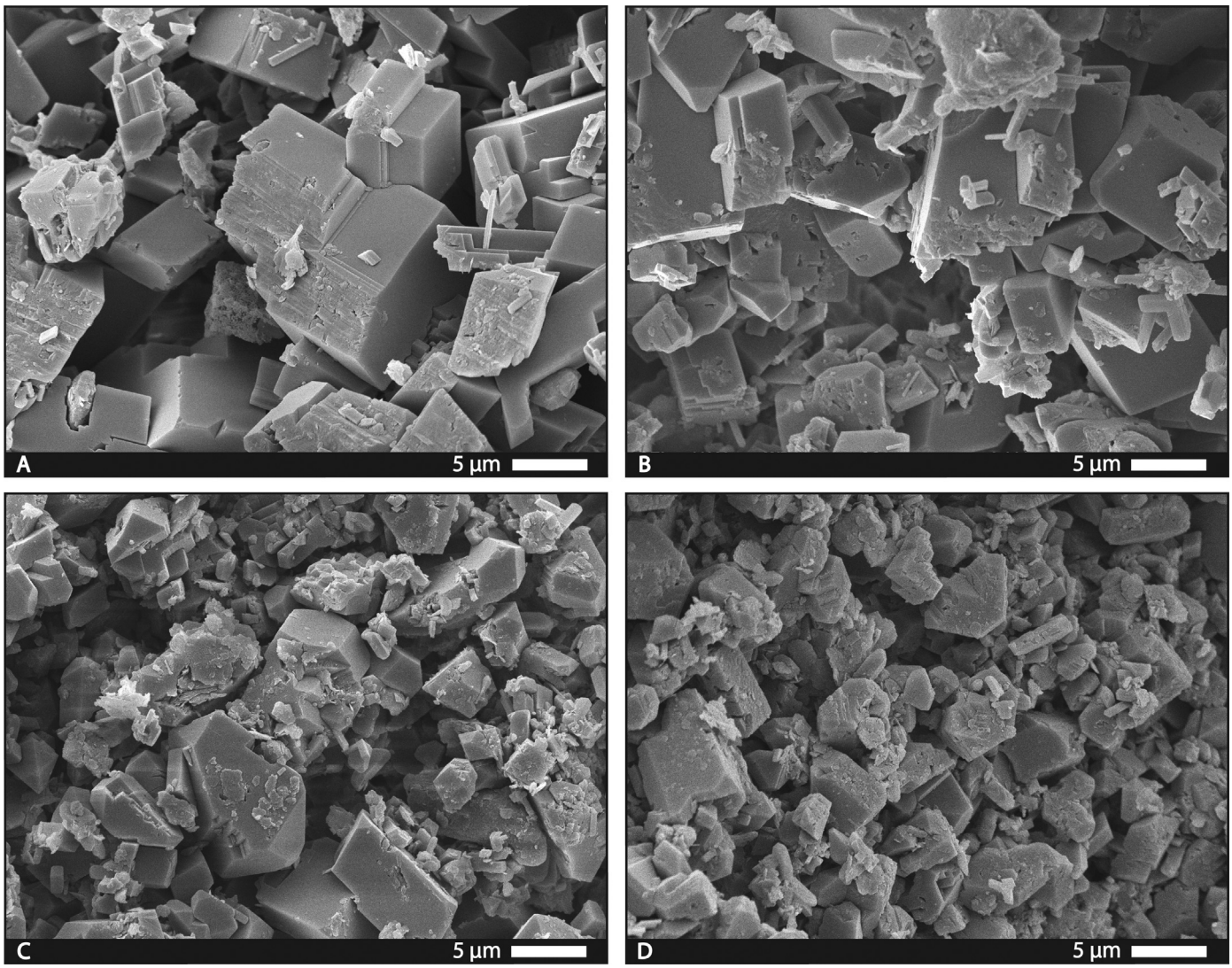

Fig. 5. SEM photomicrographs from Series 3 showing calcite microcrystals from experiments conducted with different fluid to solid ratios (mL:g). (A) 50 (5:0.1). (B) 10 (1:0.1). (C) 1 (0.1:0.1). (D) 0.8 (0.35:0.44). Note that as fluid:solid ratio decreases, the abundance of anhedral microcrystals increases while average crystal size decreases.

It is likely that the natural marine allochems examined here contained enough organic matter to impact calcite crystal texture during stabilization through substitution with CO_3^{2-} in calcite crystal lattice. Although natural marine allochems were chemically treated to eliminate organic matter, chemically treated reactants did not stabilize faster compared to untreated reactants (supplemental Fig. S6), suggesting that chemical treatment was ineffective in eliminating organic matter. The influence of organic matter on stabilization rate and calcite crystal morphology may be similar to that of SO_4^{2-}, which was inferred to substitute with CO_3^{2-} leading to retardation of reaction rate (Fig. 3c) and formation of subhedral crystals (Fig. 6c).

4.2. Controls on calcite microcrystal size and compactness

In homogenous nucleation, crystal size is controlled by an interplay between nucleation and growth rates (Genck and Larson, 1972; Myerson, 2002). The individual effect of the nucleation and growth rates on crystal size is difficult to discern, but both are incorporated in the overall reaction rate (Myerson, 2002). In heterogeneous nucleation (e.g., nucleation on a foreign surface), as it is the case here, crystal size may also be controlled by nucleation density (reactant surface area), in addition to nucleation and growth rates (Fig. 2c).

Under constant surface area (i.e., reactant size), the average crystal size (ACS) of calcite is inversely proportional to the overall reaction rate (Fig. 2d). Reaction rate in turn is controlled by temperature, fluid:solid ratio, solution chemistry, and reactant type (Fig. 3). When these variables (except reactant type) are examined individually, it is clear that they independently affect ACS and reaction rate in a similar manner, such that they increase reaction rate and yield smaller ACS compared to Series 1 (Fig. 2). Based on the understanding that higher nucleation rate produces smaller crystals because a larger number of crystals are competing for the same solutes (e.g., Ca^{2+} and CO_3^{2-}) during growth (Genck and Larson, 1972), our ACS observations suggest that temperature, fluid:solid ratio, and solution chemistry increase the nucleation rate more than the crystal growth rate.

Reaction rate and ACS from temperature, fluid:solid ratio, and $CaCl_2$ solution experiments (Series 2, 3, and 4-7) plot along a straight line (Fig. 2d), suggesting that their effect on nucleation and growth rates is similar. In contrast, reaction rate and ACS from experiments in the NaCl solution (Series 4-1) plot off the trend (ACS = 4.90 µm and overall reaction rate = 2.06% product/hour). An explanation for this discrepancy requires thorough understanding of how and why temperature, fluid:solid ratio, $CaCl_2$, and NaCl catalyze nucleation and growth rates. More specifically, what

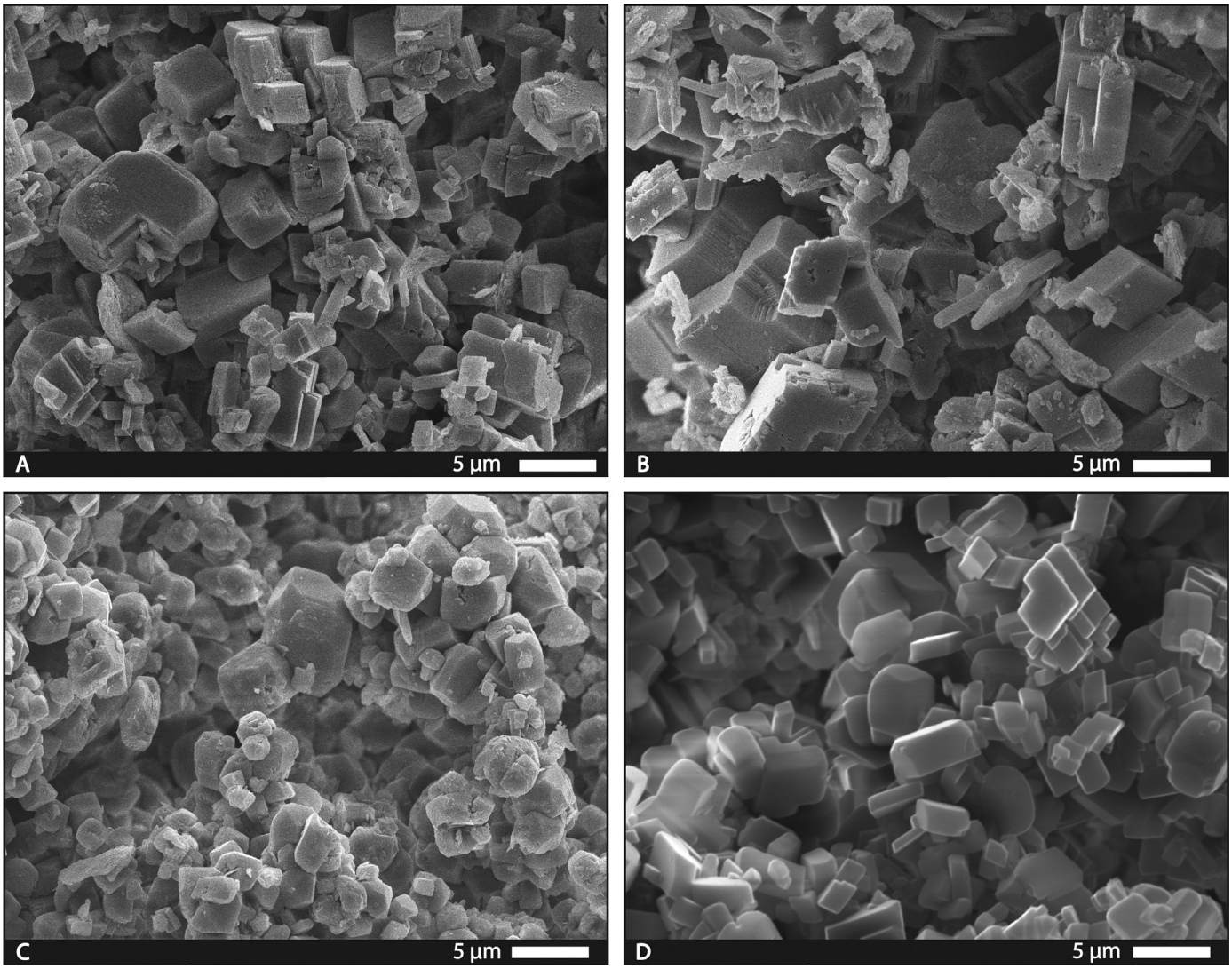

Fig. 6. SEM photomicrographs from Series 4 showing calcite microcrystals from stabilization in solutions with different chemical compositions. (A) NaCl (Series 4-1). (B) KCl (Series 4-3). (C) Na_2SO_4 (Series 4-6). (D) $CaCl_2$ (Series 4-5).

makes the effect of NaCl on reaction rate and crystal size different from other parameters? Bischoff (1968) attributed the effect of NaCl on reaction rate to the increased ionic strength of the solution, but the specific mechanism by which NaCl (and ionic strength) catalyze the reaction is still unknown and requires further investigation.

In addition to nucleation and growth rates, aragonite reactant size also exerts a measurable effect on ACS of calcite (Fig. 2c). Though not directly measured, an inverse relationship between material size and reactive surface area is well established, at least for solids with simple microstructure (e.g., Walter and Morse, 1984). Coarser reactants have less reactive surface area, which likely corresponds to a lower nucleation density, and thus limits the number of calcite crystals that can nucleate on their surface. This results in fewer, but larger crystals. In contrast, finer reactants with larger surface area are associated with a higher nucleation density, and thus result in more abundant but smaller crystals.

An important consideration is that coarser reactants correlate with slower reaction. As a result, one may attribute the observed proportional relationship between reactant size and product ACS to the slower reaction rate. However, the experiment with 90–106 µm reactant size (Series 6-1) produced calcite with an ACS of 13.28 µm, which falls off the trend between reaction rate and crystal size (Fig. 2d). This suggests that the inverse relationship observed between reactant surface area and calcite crystal size cannot be explained by the reaction rate alone, and highlights the role of nucleation density in controlling calcite crystal size.

Regarding the degree to which calcite crystals are fitted together, smaller reactants are expected to produce abundant crystals that are more closely spaced to each other due to a higher nucleation density, which can explain why experiments with smaller reactant size (<20 µm) produced fitted texture (Fig. 9b and 9c). Furthermore, surface area, and thus nucleation density, is not only controlled by reactant size, but by reactant microstructure as well (Walter and Morse, 1984). Walter and Morse (1984) showed that surface areas of some biogenic allochems, such as *Halimeda* and coral, are controlled by microstructure and surface roughness rather than by allochem size. Figure S5 highlights the differences in microstructure between the various allochems used in our experiments. In general, all aragonitic natural marine allochems are characterized by rough surfaces and complex microstructures compared to pulverized single crystal aragonite and synthetic aragonite needles (Fig. S5). Consequently, these rough surfaces of allochems contribute to a higher surface area, and thus higher nucleation density. The higher nucleation density associated with natural ma-

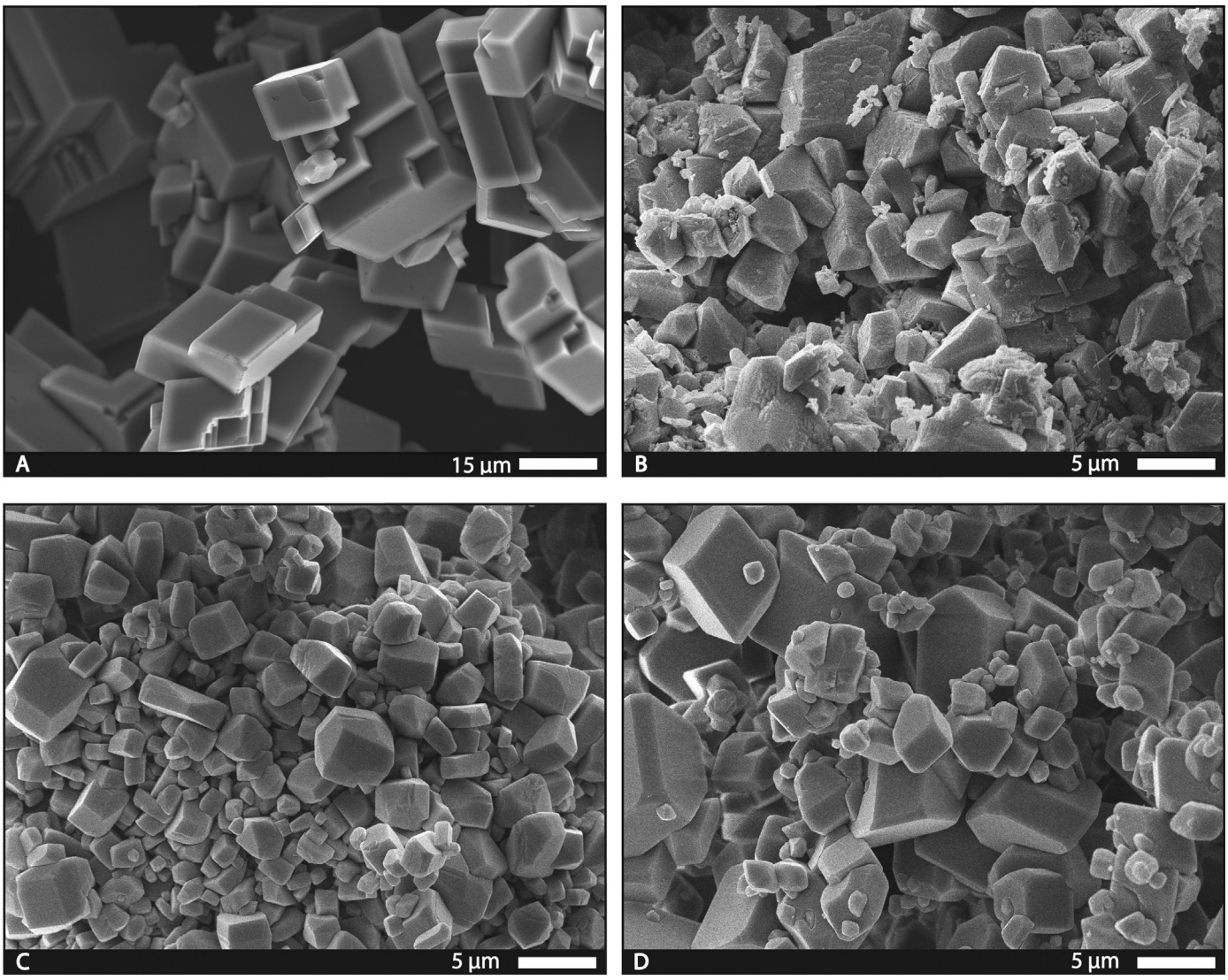

Fig. 7. SEM photomicrographs from Series 5 showing calcite microcrystals stabilized from different pulverized reactants. (A) Synthetic aragonite needles (Series 5-1). (B) Gastropods (Series 5-2). (C) Corals (Series 5-5). (D) Ooids (Series 5-6). Note that synthetic aragonite stabilized to euhedral calcite crystals, whereas natural marine allochems (B, C, and D) stabilized to subhedral (i.e., polyhedral) microcrystals.

rine allochems may explain the observation that these reactants stabilized to fitted texture (Fig. 8a, 8b, and 8c).

Reactant type also influences reaction rate and calcite crystal size (Fig. 3d, 7, and 8). However, crystal size measurements were not performed for reactant type experiments (Series 5), due to the likely influence of organic matter in natural marine allochem reactants on reaction kinetics and crystal size (section 4.1.3), which makes interpretations equivocal. Additionally, the relationship between the size of natural marine allochem reactants and their surface area is very complicated (Walter and Morse, 1984).

4.3. Implications for natural stabilization

4.3.1. Calcite microcrystal morphology and texture

Our results demonstrate that calcite microcrystal morphology, and thus texture, is determined by reactant type, fluid chemistry, and fluid:solid ratio (section 4.1). Since these variables vary significantly in natural settings (e.g., Gischler et al., 2013), inferences regarding the characteristics of precursor sediment or the diagenetic conditions of stabilization based only on calcite microcrystal texture are equivocal. However, such practices are not uncommon in literature. For example, Longman and Mench (1978) suggested that the elongated morphology of calcite microcrystals in the Cretaceous Edwards limestone emulate the shape of the aragonite needles comprising the inferred precursor sediment. Our observations show that calcite microcrystal morphology is unrelated to the morphology of the precursor aragonite. We specifically show that stabilization of aragonite needles results in euhedral calcite microcrystals (Fig. 7a). Another example is the hypothesis that stabilization in low fluid:solid ratio (i.e., closed system) produces calcite with a granular (framework) texture, whereas stabilization in high fluid:solid ratio (i.e., open system) produces calcite microcrystals with a mosaic (fitted) texture (Moshier, 1989). The implication in the open system case is that the fluid is supersaturated with respect to calcite, leading to precipitation of calcite as cement overgrowths. Our results refute this hypothesis and, instead, show that stabilization in both high and low fluid:solid ratios can yield calcite microcrystals with a granular texture (Fig. 5).

Another key implication from this study is demonstrating that textures that have previously been interpreted to indicate late diagenetic processes such as burial dissolution and cementation, may be the result of the early diagenetic process of stabilization. Lambert et al. (2006) hypothesized that rounded calcite microcrystals (i.e., granular subhedral) result from partial dissolution of the

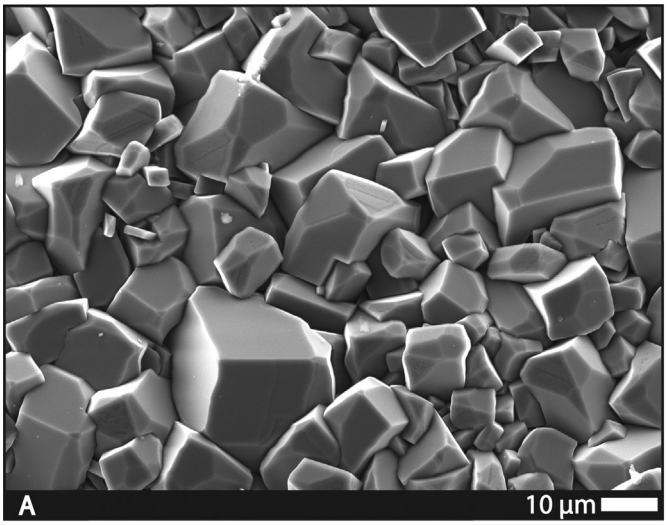

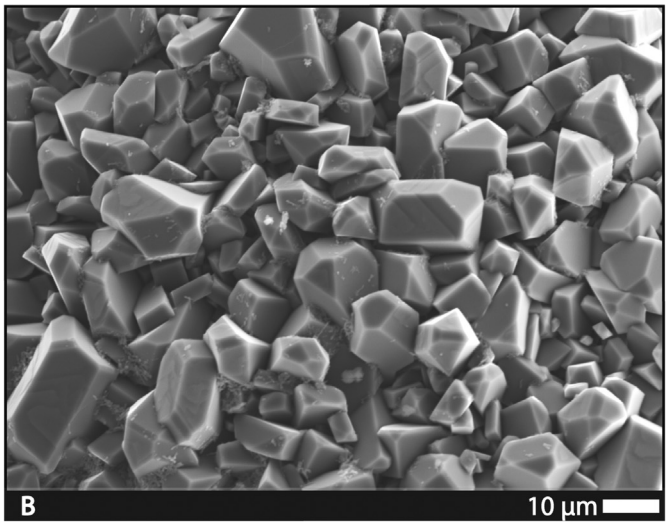

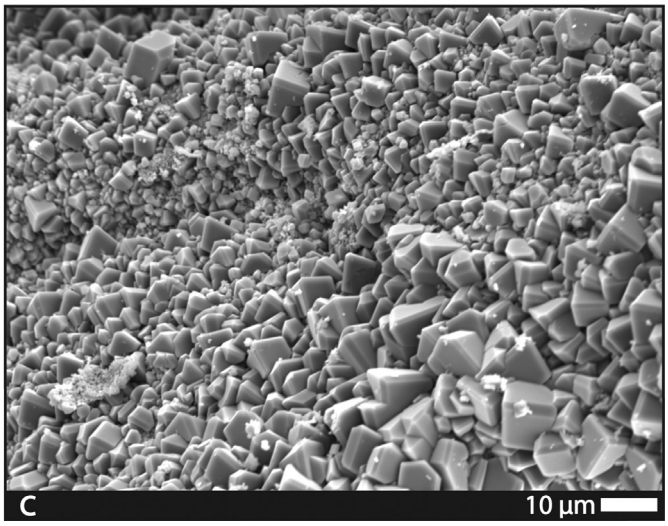

Fig. 8. SEM photomicrographs from Series 5 showing calcite microcrystals stabilized from different whole (unpowdered) reactants. (A) Corals (Series 5-7). (B) Ooids (Series 5-8). (C) *Penicillus* (Series 5-11). All reactants stabilized to subhedral microcrystals exhibiting fitted-partial texture.

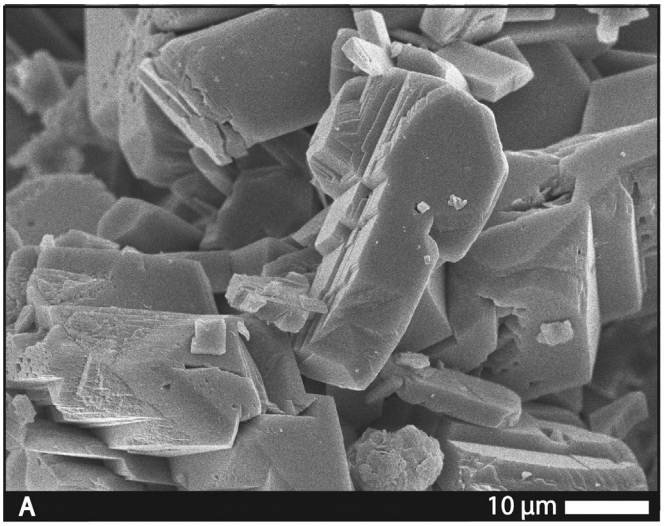

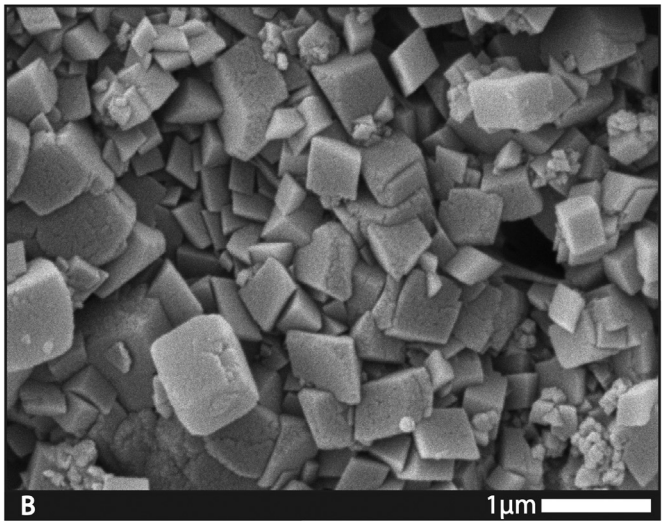

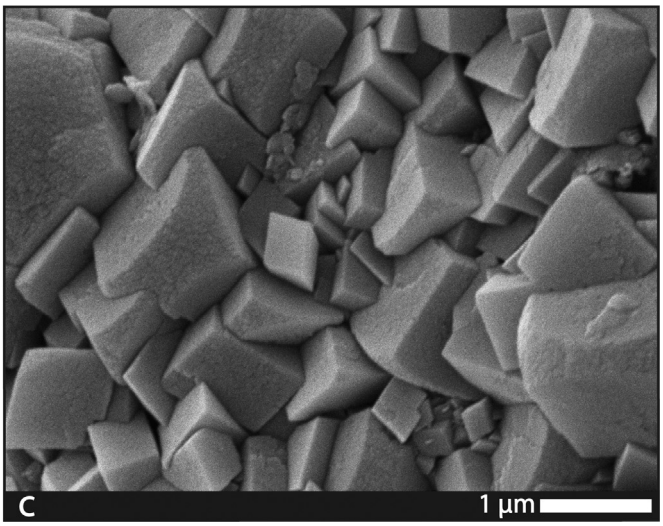

Fig. 9. SEM photomicrographs from Series 6 showing calcite microcrystals stabilized from aragonite reactants with different size fractions. (A) 90-106 µm (Series 6-1). (B) 8-20 µm (Series 6-2). (C) <8 µm (Series 6-3). All microcrystals are euhedral but larger reactants produced crystals with granular euhedral texture (A), whereas smaller reactants stabilized to crystals with fitted textures (B and C).

edges and corners of rhombic microcrystals (i.e., granular euhedral) during burial diagenesis. Observations such as rounded crystal shape, and "microgulfs and microchannels" between adjacent crystals were used as evidence for the dissolution model. This model has been extensively criticized based on theoretical (mass balance) arguments and petrographical observations (e.g., Kaczmarek et al., 2015; Ehrenberg et al., 2019). Our observations show that coral and ooid reactants stabilized to calcite microcrystals dominated by

polyhedral morphologies and exhibited bimodality (Fig. 7c and 7d). Moreover, stabilization of aragonite in $CaCl_2$ solution yields a few polyhedral calcite microcrystals (Fig. 6d). These observations indicate that polyhedral calcite microcrystals can result directly from stabilization of metastable sediments, which offers an alternative diagenetic model to forming this common calcite microcrystal texture.

The suggestion that fitted textures indicate cementation due to compaction (e.g., Lambert et al., 2006; Volery et al., 2010; Deville de Periere et al., 2011) is based on the observed association between fitted texture, stylolitization, and epitaxial overgrowth cement. Our observations show that fitted textures can be produced during stabilization of natural marine allochems such as corals, ooids, and *Penicillus* (Fig. 8 and S3) and the ultra-fine single crystal aragonite (Fig. 9b and 9c). What is common between these two experiments is that fine reactants and marine allochems are both characterized by high surface area, which results in high nucleation density, and thus closely spaced (i.e., fitted) calcite microcrystals (section 4.2). The fitted textures that result during stabilization are similar to the compact anhedral texture of Lambert et al. (2006), and the meshed microfabric texture of Volery et al. (2010). Based on these observations, at least some fitted textures can be produced during stabilization, and may not require burial compaction.

4.3.2. Calcite microcrystal size

Our results show that calcite microcrystal size is controlled by temperature, fluid:solid ratio, fluid chemistry, and reactant size (section 4.2). Additionally, precursor mineralogy (aragonite vs. HMC) has been proposed by Lasemi and Sandberg (1993) to control calcite microcrystal size. They reasoned that calcite nucleates more readily on HMC, which would result in smaller microcrystals, compared to aragonite. These observations imply that, in ancient limestones, it is challenging to determine the controls on calcite microcrystal size. An attempt has been made by Deville de Periere et al. (2011), who observed that coarser calcite microcrystals were associated with rudist-rich bioclastic facies, whereas finer microcrystals were associated with muddier facies. They suggested that calcite microcrystal size may be determined by the depositional hydrodynamic conditions. Perhaps, the implication here is that calcite microcrystals are depositional in origin, since the studied limestones were Cretaceous and thus precipitated during "calcite seas" (Sandberg, 1983). Another way to interpret the observations of Deville de Periere et al. is that precursor sediment with smaller size fractions are characterized by larger surface area (high nucleation density), thus yields smaller calcite microcrystals, whereas sediment with larger size fractions yield larger microcrystals (Fig. 9). It is important to note that Deville de Periere et al. (2011) stated that the relationship between calcite microcrystal size and depositional environments is observed in some intervals, but it falls apart in other intervals. This observation may attest to the difficulty of preservation of such relationships in the rock record, and perhaps to the possible control on crystal size by other depositional and diagenetic variables.

Large calcite crystals (i.e., microspar) are often suggested to have formed from smaller calcite microcrystals (i.e., micrite) through aggrading neomorphism (e.g., Bathurst, 1975; Volery et al., 2010; Morad et al., 2018). Conceptually, aggrading neomorphism is similar to Ostwald ripening (Morse and Casey, 1988), and the two terms have been used interchangeably. In principle, smaller particles (e.g., crystals) are more soluble compared to larger particles due to the contribution of surface free energy (Morse and Casey, 1988), and should consequently recrystallize to larger crystals with time. For carbonates, however, the influence of particle size on solubility is only significant for particles whose diameter is <0.1 µm and decreases exponentially with increasing particle size (Morse and Mackenzie, 1990). What this means is that Ostwald ripening rate (i.e., dissolution rate) is a function of initial crystal size. Morse and Mackenzie (1990) calculated the rate of Ostwald ripening in seawater at 25 °C, and showed that calcite crystals with 1 µm diameter would take 1 billion years to dissolve, whereas 0.1 µm crystals would dissolve in 100,000 years. Our results (Series 1) are consistent with these calculations and show that aragonite stabilizes to calcite with an average crystal size (ACS) of 5.28 µm and does not increase with extended reaction time (Fig. 2a). Therefore, aggrading neomorphism (i.e., Ostwald ripening) does not appear to be operative on calcite microcrystals that result from stabilization, probably because the initial crystal size is large, and thus the contribution of surface free energy to solubility is insignificant. However, we measured ACS with reaction time only for experiments with <63 µm reactants (Series 1). It should be noted that experiments with finer reactants (Series 6-2 and 6-3) produced smaller ACS compared to Series 1 (Fig. 2c). Such fine crystals are expected to be more susceptible to Oswald ripening.

4.4. The applicability of experiments to natural settings and the path forward

Since aragonite to calcite stabilization rate at room temperature is too slow (e.g., McManus, 1982), higher temperatures are required to stabilize aragonite in a reasonable period of time. However, reaction mechanism may differ as a function of temperature, and consequently stabilization in the laboratory may not reflect stabilization in nature (Morse and Mackenzie, 1990). The dependence of reaction mechanism on temperature can be determined using Arrhenius plot. This analysis has previously been performed by several authors (e.g., Taft, 1967; Bischoff, 1969; McManus, 1982), who concluded that the aqueous transformation of aragonite to calcite is characterized by the same reaction mechanism across the range of temperature examined (50–300 °C) (see review by McManus, 1982). Furthermore, Vahrenkamp et al. (2014) used clumped isotopes to determine the temperature at which stabilization occurred in a Cretaceous limestone and inferred a temperature between 59–72 °C. Another observation that is consistent with the hypothesis that similar reaction mechanisms operate in experimental and natural stabilization is the textural similarities between calcite produced from experiments and calcite in nature. These observations indicate that using a reaction temperature of 70 °C in experiments is justified, and that conclusions reached from experiments regarding calcite microcrystal textures are relevant to natural systems.

The observations that calcite microcrystal texture is controlled by various depositional and diagenetic conditions, and that these conditions vary considerably in nature have two implications. First, generalizations regarding the diagenetic origin of calcite microtextures based on limited case studies are unwarranted. Second, understanding the diagenetic history of calcite microcrystal textures requires comprehensive evaluation of local conditions. Furthermore, this and other studies (e.g., McManus, 1982; Papenguth, 1991; Casella et al., 2017; Pederson et al., 2019) have shown that the experimental approach provides invaluable insights into the diagenesis of calcite microtextures. Further experimental work is needed to evaluate other textural controls, such as organic matter and trace elements in aragonite reactants, on calcite during stabilization. Finally, we show here that polyhedral calcite microcrystals can form during stabilization. It is still undetermined whether polyhedral crystals can form via dissolution of euhedral calcite crystals as previously suggested (Lambert et al., 2006).

5. Conclusions

Aragonite stabilization experiments produce low-magnesium calcite microcrystals exhibiting textures remarkably similar to

those commonly observed in the rock record. Calcite microtextures are impacted by various depositional and diagenetic parameters. Calcite microcrystal morphology is controlled by fluid chemistry, fluid:solid ratio, and reactant type, whereas calcite microcrystal size is controlled by temperature, fluid:solid ratio, fluid chemistry, and reactant size. The degree to which these calcite microcrystals are fitted together, in contrast, is controlled by reactant size and reactant microstructure.

These findings show that although aragonite to calcite stabilization is a simple mineral replacement reaction, the process is complicated owing to the variations in types, sizes, and textures of aragonitic sediments in nature, and the various diagenetic conditions under which stabilization occurs. This study challenges most of the existing hypotheses regarding the origin of calcite microcrystal textures. Specifically, we show that textures that have been interpreted to indicate late diagenetic processes such as dissolution and cementation, may be the result of the early diagenetic process of stabilization.

Declaration of competing interest

The authors declare that they have no known competing financial interests or personal relationships that could have appeared to influence the work reported in this paper.

Acknowledgements

This study was supported by a grant from the U.S. National Science Foundation awarded to SEK (EAR-SGP-1828880). We are thankful to the two anonymous reviewers for their helpful comments and suggestions. We would like to thank our colleagues in the Carbonate Petrology and Characterization Laboratory Cameron Manche, Katharine Rose, and Sara Hayes for constructive criticism on earlier versions of this manuscript. Zander Sorenson acquired the crystal size measurements. Amy Albin and Aby Vanderberg at MSU provided assistance with SEM imaging. Michelle Gannon at Drexel University and Abubkr Abuhagr at the department of Chemistry at WMU helped with loss on ignition preliminary experiments.

Appendix A. Supplementary material

Supplementary material related to this article can be found online at https://doi.org/10.1016/j.epsl.2020.116235.

References

Ahm, A.S.C., Bjerrum, C.J., Blättler, C.L., Swart, P.K., Higgins, J.A., 2018. Quantifying early marine diagenesis in shallow-water carbonate sediments. Geochim. Cosmochim. Acta 236, 140–159.

Bathurst, 1975. Carbonate Sediments and Their Diagenesis. Developments in Sedimentology, vol. 12. Elsevier, p. 658.

Bischoff, J.L., 1968. Kinetics of calcite nucleation: magnesium ion inhibition and ionic strength catalysis. J. Geophys. Res. 73 (10), 3315–3322.

Bischoff, J.L., 1969. Temperature controls on aragonite-calcite transformation in aqueous solution. Am. Mineral., J. Earth Planet. Mater. 54 (1–2), 149–155.

Bischoff, J.L., Fyfe, W.S., 1968. Catalysis, inhibition, and the calcite-aragonite problem; [Part] 1, the aragonite-calcite transformation. Am. J. Sci. 266 (2), 65–79.

Bosak, T., Newman, D.K., 2005. Microbial kinetic controls on calcite morphology in supersaturated solutions. J. Sediment. Res. 75 (2), 190–199.

Busenberg, E., Plummer, L.N., 1985. Kinetic and thermodynamic factors controlling the distribution of SO_4^{2-} and Na^+ in calcites and selected aragonites. Geochim. Cosmochim. Acta 49 (3), 713–725.

Casella, L.A., Griesshaber, E., Yin, X., Ziegler, A., Mavromatis, V., Müller, D., Ritter, A.-C., Hippler, D., Harper, E.M., Dietzel, M., Immenhauser, A., Schöne, B.R., Angiolini, L., Schmahl, W.W., 2017. Experimental diagenesis: insights into aragonite to calcite transformation of Arctica islandica shells by hydrothermal treatment. Biogeosciences 14, 1461–1492. https://doi.org/10.5194/bg-14-1461-2017.

Deville de Periere, M., Durlet, C., Vennin, E., Lambert, L., Caline, B., Bourillot, R., Poli, E., 2011. Morphometry of micrite particles in Cretaceous microporous limestones of the middle East: influence on reservoir properties. Mar. Pet. Geol. 28, 1727–1750. https://doi.org/10.1016/j.marpetgeo.2011.05.002.

Ehrenberg, S.N., Walderhaug, O., Bjørlykke, K., 2019. Discussion of "Microfacies, diagenesis and oil emplacement of the Upper Jurassic Arab-D carbonate reservoir in an oil field in central Saudi Arabia (Khurais Complex)" by Rosales et al. (2018). Mar. Pet. Geol. 100, 551–553.

Folk, R.L., 1974. The natural history of crystalline calcium carbonate; effect of magnesium content and salinity. J. Sediment. Res. 44 (1), 40–53.

Genck, W.J., Larson, M.A., 1972. Temperature effects of growth and nucleation rates in mixed suspension crystallization. In: Estrin, J. (Ed.), Crystallization from Solution: Nucleation Phenomena in Growing Crystal Systems. In: Symposium Series, No. 121, vol. 68. American Institute of Chemical Engineers, pp. 57–66.

Gischler, E., Dietrich, S., Harris, D., Webster, J.M., Ginsburg, R.N., 2013. A comparative study of modern carbonate mud in reefs and carbonate platforms: mostly biogenic, some precipitated. Sediment. Geol. 292, 36–55.

Guo, Y., Deng, W., Wei, G., 2019. Kinetic effects during the experimental transition of aragonite to calcite in aqueous solution: insights from clumped and oxygen isotope signatures. Geochim. Cosmochim. Acta 248, 210–230.

Hashim, M.S., Kaczmarek, S.E., 2019. A review of the nature and origin of limestone microporosity. Mar. Pet. Geol. 107, 527–554.

Hasiuk, F.J., Kaczmarek, S.E., Fullmer, S.M., 2016. Diagenetic origins of the calcite microcrystals that host microporosity in limestone reservoirs. J. Sediment. Res. 86 (10), 1163–1178.

Ishikawa, M., Ichikuni, M., 1984. Uptake of sodium and potassium by calcite. Chem. Geol. 42 (1–4), 137–146.

Jackson, T.A., Bischoff, J.L., 1971. The influence of amino acids on the kinetics of the recrystallization of aragonite to calcite. J. Geol. 79 (4), 493–497.

Kaczmarek, S.E., Fullmer, S.M., Hasiuk, F.J., 2015. A universal classification scheme for the microcrystals that host limestone microporosity. J. Sediment. Res. 85, 1197–1212.

Katz, A., 1973. The interaction of magnesium with calcite during crystal growth at 25–90 °C and one atmosphere. Geochim. Cosmochim. Acta 37 (6), 1563–1586.

Kominz, M.A., Patterson, K., Odette, D., 2011. Lithology dependence of porosity in slope and deep marine sediments. J. Sediment. Res. 81 (10), 730–742.

Lambert, L., Durlet, C., Loreau, J.P., Marnier, G., 2006. Burial dissolution of micrite in middle East carbonate reservoirs (Jurassic-Cretaceous): keys for recognition and timing. Mar. Pet. Geol. 23, 79–92.

Lasemi, Z., Sandberg, P., 1993. Microfabric and compositional clues to dominant mud mineralogy of micrite precursors. In: Carbonate Microfabrics. Springer, New York, NY, pp. 173–185.

Longman, M.W., Mench, P.A., 1978. Diagenesis of Cretaceous limestones in the Edwards aquifer system of south-central Texas: a scanning electron microscope study. Sediment. Geol. 21 (4), 241–276.

Loucks, R.G., Lucia, F.J., Waite, L.E., 2013. Origin and description of the micropore network within the Lower Cretaceous Stuart City Trend tight-gas limestone reservoir in Pawnee Field in south Texas. GCAGS J. 2, 29–41.

Lowenstein, T.K., Timofeeff, M.N., Brennan, S.T., Hardie, L.A., Demicco, R.V., 2001. Oscillations in Phanerozoic seawater chemistry: evidence from fluid inclusions. Science 294 (5544), 1086–1088.

McManus, K.M., 1982. The aqueous aragonite to calcite transformation: rate, mechanisms, and its role in the development of neomorphic fabrics. Master's Thesis. Virginia Polytechnic Institute and State University.

McManus, K.M., Rimstidt, J.D., 1982. Aqueous aragonite to calcite transformation: a geometry controlled dissolution-precipitation reaction (abstract). Geol. Soc. Am. Abstr. Program 14, 562.

Millero, F.J., 2016. Chemical Oceanography. CRC Press.

Milliman, J.D., 1974. Marine Carbonates, Part I. Heidelberg Springer-Verlag, Berlin, Heidelberg.

Morad, D., Paganoni, M., Al Harthi, A., Morad, S., Ceriani, A., Mansurbeg, H., Al Suwaidi, A., Al-Aasm, I.S., Ehrenberg, S.N., 2018. Origin and evolution of microporosity in packstones and grainstones in a Lower Cretaceous carbonate reservoir, United Arab Emirates. Geol. Soc. (Lond.) Spec. Publ. 435 (1), 47–66.

Morse, J.W., 1986. The surface chemistry of calcium carbonate minerals in natural waters: an overview. Mar. Chem. 20 (1), 91–112.

Morse, J.W., Casey, W.H., 1988. Ostwald processes and mineral paragenesis in sediments. Am. J. Sci. 288 (6), 537–560.

Morse, J.W., Mackenzie, F.T., 1990. Geochemistry of Sedimentary Carbonates (Vol. 48). Elsevier.

Morse, J.W., Arvidson, R.S., Lüttge, A., 2007. Calcium carbonate formation and dissolution. Chem. Rev. 107 (2), 342–381.

Moshier, S.O., 1989. Microporosity in micritic limestones: a review. Sediment. Geol. 63 (3–4), 191–213.

Myerson, A., 2002. Handbook of Industrial Crystallization. Butterworth-Heinemann.

Oti, M., Müller, G., 1985. Textural and mineralogical changes in coralline algae during meteoric diagenesis-an experimental approach. Neues Jahrb. Mineral. Abh. 151 (2), 163–195.

Papenguth, H.W., 1991. Experimental diagenesis of lime mud. Doctoral dissertation. University of Illinois at Urbana-Champaign.

Pederson, C., Mavromatis, V., Dietzel, M., Rollion-Bard, C., Nehrke, G., Neuser, R., Jöns, N., Jochum, K.P., Immenhauser, A., 2019. Diagenesis of mollusc aragonite and the role of fluid reservoirs. Earth Planet. Sci. Lett. 514, 130–142.

Perdikouri, C., Piazolo, S., Kasioptas, A., Schmidt, B.C., Putnis, A., 2013. Hydrothermal replacement of aragonite by calcite: interplay between replacement, fracturing and growth. Eur. J. Mineral. 25 (2), 123–136.

Ritter, A.C., Mavromatis, V., Dietzel, M., Kwiecien, O., Wiethoff, F., Griesshaber, E., Casella, L.A., Schmahl, W.W., Koelen, J., Neuser, R.D., Leis, A., 2017. Exploring the impact of diagenesis on (isotope) geochemical and microstructural alteration features in biogenic aragonite. Sedimentology 64 (5), 1354–1380.

Roduit, N., 2007. Un logiciel d'analyse d'images pétrographiques polyvalent. Doctoral dissertation. University of Geneva.

Sandberg, P.A., 1983. An oscillating trend in Phanerozoic non-skeletal carbonate mineralogy. Nature 305 (5929), 19.

Sunagawa, I., 2007. Crystals: Growth, Morphology, & Perfection. Cambridge University Press.

Taft, W.H., 1967. Physical Chemistry of Formation of Carbonates. Developments in Sedimentology, vol. 9. Elsevier, pp. 151–167.

Vahrenkamp, V., Barata, J., Van Laer, P.J., Swart, P., Murray, S., 2014. Micro rhombic calcite of a Giant Barremian (Thamama B) reservoir onshore Abu Dhabi-clumped isotope analyses fix temperature, water composition and timing of burial diagenesis. In: Abu Dhabi International Petroleum Exhibition and Conference. Society of Petroleum Engineers.

Volery, C., Davaud, E., Foubert, A., Caline, B., 2010. Lacustrine microporous micrites of the Madrid Basin (Late Miocene, Spain) as analogues for shallow-marine carbonates of the Mishrif reservoir Formation (Cenomanian to Early Turonian, Middle East). Facies 56 (3), 385–397.

Walter, L.M., Morse, J.W., 1984. Reactive surface area of skeletal carbonates during dissolution; effect of grain size. J. Sediment. Res. 54 (4), 1081–1090.

Wray, J.L., Daniels, F., 1957. Precipitation of calcite and aragonite. J. Am. Chem. Soc. 79 (9), 2031–2034.